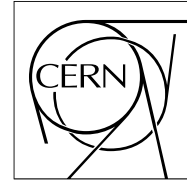




The Compact Muon Solenoid Experiment

CMS Performance Note

Mailing address: CMS CERN, CH-1211 GENEVA 23, Switzerland



20 November 2024

Level-1 Trigger Performance in 2024 Proton-Proton Collisions at $\sqrt{s} = 13.6$ TeV

CMS Collaboration

Abstract

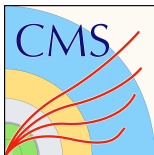
In 2024, the CMS experiment collected a record-large data set of proton-proton collisions at $\sqrt{s} = 13.6$ TeV, corresponding to an integrated luminosity of 114 fb^{-1} . This note summarizes the performance of the CMS Level-1 Trigger system to identify and select muons, jets, transverse energy sums, electrons/photons, and hadronically decaying tau leptons in this data set.

Level-1 Trigger Performance in 2024 Proton-Proton Collisions at $\sqrt{s} = 13.6$ TeV

CMS Collaboration

`cms-dpg-conveners-l1t@cern.ch`

<https://twiki.cern.ch/twiki/bin/view/CMSPublic/L1TriggerDPGResults>



Abstract

In 2024, the CMS experiment collected a record-large data set of proton-proton collisions at $\sqrt{s} = 13.6$ TeV, corresponding to an integrated luminosity of 114 fb^{-1} . This note summarizes the performance of the CMS Level-1 Trigger system to identify and select muons, jets, transverse energy sums, electrons/photons, and hadronically decaying tau leptons in this data set.

Level-1 Trigger Rate Allocation

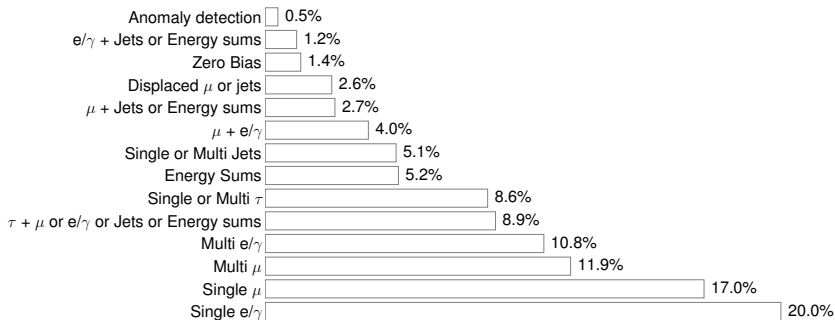


Figure 1: Fractions of the ≈ 110 kHz total rate of the CMS Level-1 Trigger (L1T) allocated for single- and multi-object triggers, cross triggers, generic zero-bias triggers, and anomaly detection triggers, in a typical CMS physics menu during the 2024 proton-proton collision data taking.

Jets & Energy Sums

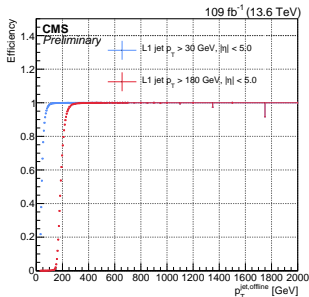
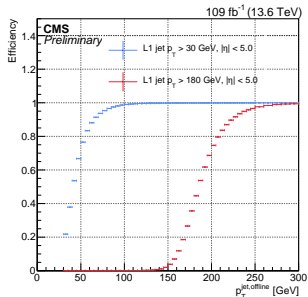
Jets & Transverse Energy Sums: Reconstruction

- ▶ L1T jets are reconstructed starting from the electromagnetic and hadronic calorimeter energy deposits, grouped together in Trigger Towers (TT) and characterized by η , ϕ and transverse energy (E_T) [1, 2]. A jet is formed by gathering all TTs in a 9×9 grid in the η and ϕ directions, and the energy associated with pileup interactions is subtracted. Jet energy corrections are then applied to calibrate the jet E_T .
- ▶ HTT is defined as the scalar E_T sum of the L1T jets within $|\eta| < 2.5$ and with corrected $E_T > 30$ GeV.

Jets & Transverse Energy Sums: Efficiency Measurement

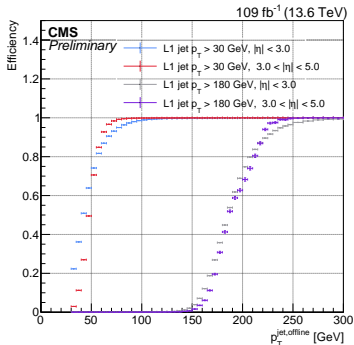
- ▶ Collision events having an isolated muon with $p_T > 24$ GeV reconstructed at the high-level trigger are selected for measuring the L1T jet, HTT, and ETMHF efficiencies.
- ▶ The events must contain at least one offline reconstructed muon passing stringent identification and isolation requirements, with $p_T > 25$ GeV and $|\eta| < 2.4$.
- ▶ Any event with poorly reconstructed low energy muons are discarded to reduce contamination in offline jet reconstruction.
- ▶ The events must have at least one offline reconstructed jet having $p_T > 30$ GeV that satisfies strict identification requirements and contains low quantities of muon and electromagnetic energy fraction.

L1T Jet Efficiency



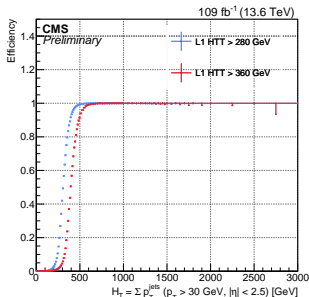
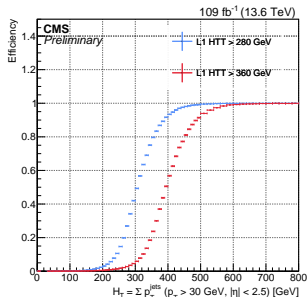
- ▶ L1T jet efficiency as a function of offline-reconstructed jet p_T , for L1T p_T thresholds of 30 GeV (blue) and 180 GeV (red).
- ▶ Denominator: Offline jets with $p_T > 15$ GeV and $|\eta| < 5.0$
- ▶ Numerator: Offline jets with $p_T > 15$ GeV and $|\eta| < 5.0$ and spatially matched to a L1T jet within $\Delta R < 0.4$

L1T Jet Efficiency



- ▶ Comparison of L1T jet efficiency as a function of offline jet p_T for L1T p_T thresholds of 30 GeV (blue and red) and 180 GeV (gray and purple) for pseudorapidity regions $|\eta| < 3.0$ (blue and gray) and $3.0 < |\eta| < 5.0$ (red and purple). The former contains the overlap region between the endcap and forward calorimeters ($2.5 < |\eta| < 3.0$), where the turn-on is slow, causing the $|\eta| < 3.0$ turn-ons to look slower in comparison.

HTT Efficiency



- ▶ L1T HTT Efficiency as a function of the corresponding offline-reconstructed jet p_T sum (H_T), for HTT thresholds of 280 GeV (blue) and 360 GeV (red).
- ▶ H_T is reconstructed as a scalar sum of all offline jets with $p_T > 30 \text{ GeV}$ and $|\eta| < 2.5$, excluding jets matched to muons.
- ▶ Denominator: Single-muon events selected as described above.
- ▶ Numerator: All selected single-muon events where the L1T HTT values exceed the chosen threshold.

Muons

L1T Muons: Reconstruction & Identification

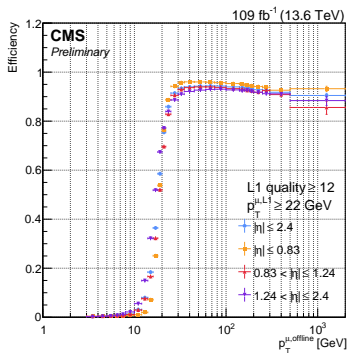
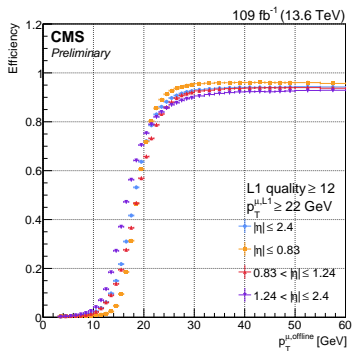
- ▶ The Level-1 muon trigger consists of three separate track finders: Barrel Muon track finder (BMTF) covering $|\eta| < 0.83$, Overlap Muon track finder (OMTF) covering $0.83 < |\eta| < 1.24$ and Endcap Muon track finder (EMTF) covering $1.24 < |\eta| < 2.4$.
- ▶ All three systems send muon candidates to the Global Muon Trigger (μ GMT), which is responsible for sorting in p_T & quality and for removing duplicate muons.
- ▶ L1T muon quality ranges from 0 to 15. Muons with quality ≥ 4 are labeled "open quality" and are used in special triggers, quality ≥ 8 are labeled "double quality" and are used in standard multi-muon triggers, quality ≥ 12 are labeled "single quality" and are used in single-muon triggers, and quality values ≥ 14 represent the new "very high quality" muons which are used in barrel-only low- p_T muon triggers.

L1T Muon Efficiency Measurement: Tag & Probe Method

- ▶ The efficiency of the L1T muon trigger is measured using the tag-and-probe method and the following selections on offline-reconstructed muons.

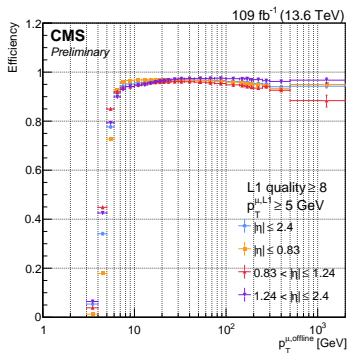
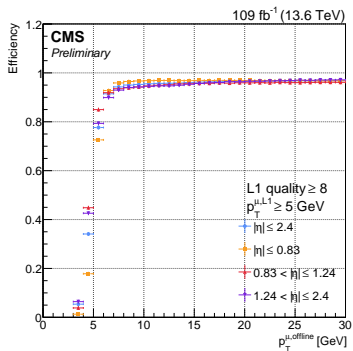
Tag muon	Probe muon	Tag-and-probe selection
$ \eta < 2.4$ Tight ID Matched to an isolated HLT muon $\Delta R(\text{HLT, offline}) < 0.1$ $p_T \geq 27 \text{ GeV}$ Relative isolation < 0.15	$ \eta < 2.4$ Tight ID $\Delta R(\text{L1, offline}) < 0.2$ Relative isolation < 0.15	$\Delta R(\text{tag, probe}) > 0.4$

Muon Efficiency vs. p_T



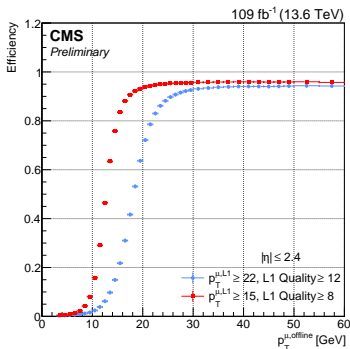
- ▶ L1T muon efficiency as a function of offline-reconstructed muon p_T , for L1T muon p_T threshold of 22 GeV and L1T quality cut 12, separately for each track finder and combined.

Muon Efficiency vs. p_T



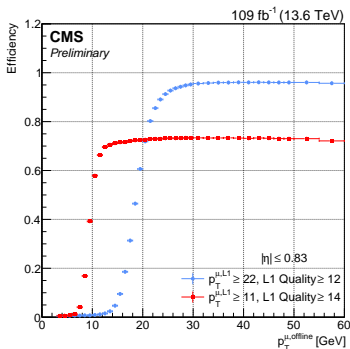
- ▶ L1T muon efficiency as a function of offline-reconstructed muon p_T , for L1T muon p_T threshold of 5 GeV and L1T quality cut 8, separately for each track finder and combined.

Muon Efficiency vs. p_T and Quality



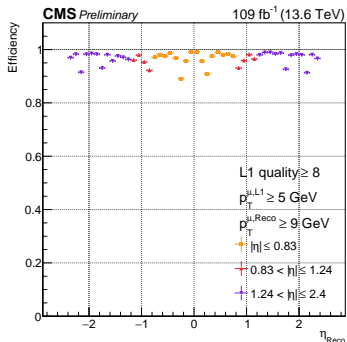
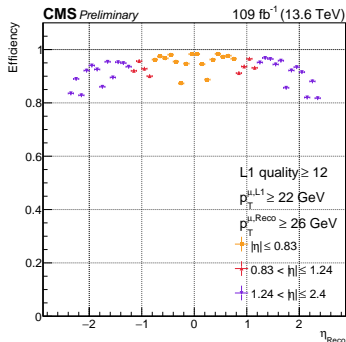
- ▶ Efficiency vs p_T for μ GMT L1T muons with L1T quality cuts at 12 and 8 and p_T cuts at 22 GeV and 15 GeV, respectively.

Muon Efficiency vs. p_T



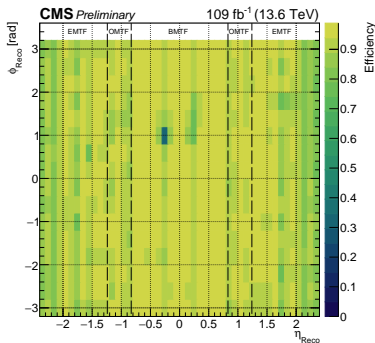
- ▶ Efficiency vs p_T for BMTF L1T muons with L1T quality cuts at 12 and 14 in the p_T range 0 – 60 GeV. A p_T cut at 22 GeV and 11 GeV was used respectively. The new "very high quality" working point is chosen to have very high L1T muon purity and recovers muons in low p_T region while staying within the available L1T rate budget.

Muon Efficiency vs η



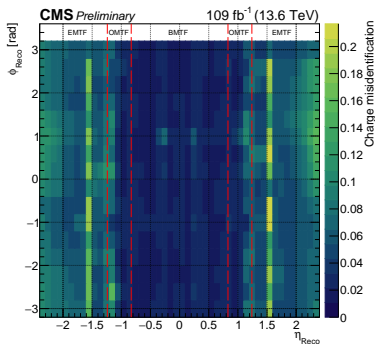
- ▶ Efficiency vs η for L1T muons with L1T p_{T} cuts of 22 GeV (left) and 5 GeV (right), offline p_{T} cuts of 26 GeV (left) and 9 GeV (right), and L1T quality cuts of 12 (left) and 8 (right) for each track finder. Efficiency drops near $|\eta| \approx 0.3$ and $|\eta| \approx 0.8$ are due to gaps between wheels ($\pm 0, \pm 1$ and $\pm 1, \pm 2$), while efficiency drops near $|\eta| \approx 1.6$ and $|\eta| \approx 2.1$ are due to gaps between endcap muon detector rings and detector specific features, respectively.

Muon Efficiency vs $\eta - \phi$



- ▶ Efficiency vs $\eta - \phi$ for L1T muons with L1T p_T at 22 GeV, an offline p_T cut at 26 GeV and a quality cut at 12. The drop in efficiency at $(\eta, \phi) \approx (-0.3, 1)$ is due to the cables passing through the detector.

Muon Charge Misidentification



- ▶ 2D η - ϕ plot of L1T muon charge misidentification. L1T muons are matched to offline muons if $\Delta R(\text{L1}, \text{offline}) < 0.1$. Regions at $|\eta| = \pm 1.5$ with some charge misidentification are present due to overlapping detector regions. Remaining regions of higher charge misidentification are due to residual misalignment in muon detectors.

Electrons & photons (e/γ)

L1T e/γ : Reconstruction & Identification

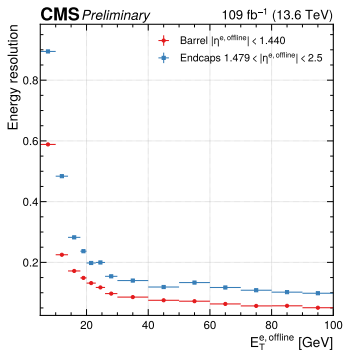
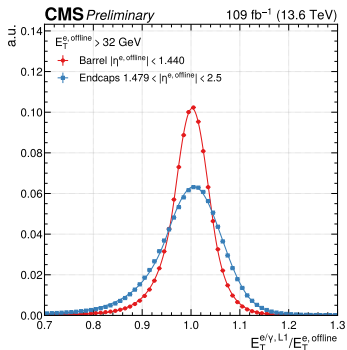
- ▶ The e/γ candidates are reconstructed from calorimeter TTs by clustering TTs around a “seed” defined as a local transverse energy (E_T) maximum above 2 GeV.
- ▶ Clusters are built dynamically, i.e. including surrounding TTs with $E_T \geq 1$ GeV without any predetermined cluster shape requirement, and then trimmed.
- ▶ The e/γ candidates are subject to identification criteria such as shape and HCAL over ECAL energy deposit fraction.
- ▶ Isolation requirements are finally added to produce a collection of isolated e/γ objects. The isolation transverse energy E_T^{Iso} corresponds to the energy deposit in a 6×9 TTs region in $\eta \times \phi$ around the seed TT, subtracting the candidate E_T . To determine if a candidate is isolated, a selection threshold is applied to E_T^{Iso} depending on the candidate E_T , its η position, and a pileup estimator.
- ▶ The candidate E_T is then subject to further calibration, depending on the candidate E_T , its η position, and its shape.

L1T e/γ : Efficiency measurement

- ▶ The efficiency of the L1T e/γ trigger is measured using the tag-and-probe method and the following selections on offline-reconstructed electrons.

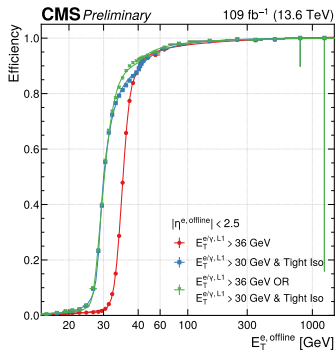
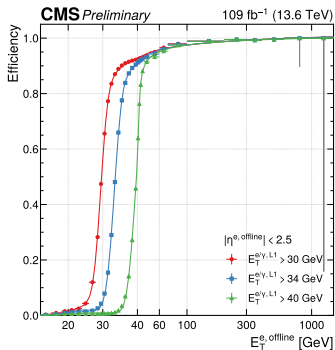
Tag electron	Probe electron	Tag-and-probe selection
$ \eta < 2.5$ Medium ID Matched to an isolated HLT electron firing the single-electron HLT path with threshold $p_T > 32 \text{ GeV}$ $\Delta R(\text{HLT, offline}) < 0.3$ $p_T > 30 \text{ GeV}$	$ \eta < 2.5$ Loose ID	$\Delta R(\text{tag, probe}) > 0.6$ $60 < m_{ee} < 120 \text{ GeV}$ $m_T < 30 \text{ GeV}$

e/γ : Energy response and resolution



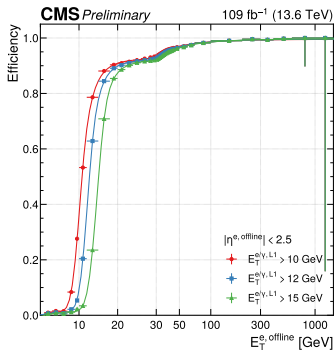
- ▶ Left: The L1T e/γ trigger energy response with respect to the offline reconstructed E_T , for the barrel and endcap regions.
- ▶ Right: The L1T e/γ trigger energy resolution, as a function of the $E_T^{e, \text{offline}}$, estimated by the root-mean-square of the $E_T^{e/\gamma, L1} / E_T^{e, \text{offline}}$ distribution divided by its mean, in bins of $E_T^{e, \text{offline}}$.

e/γ : Efficiency vs. p_T



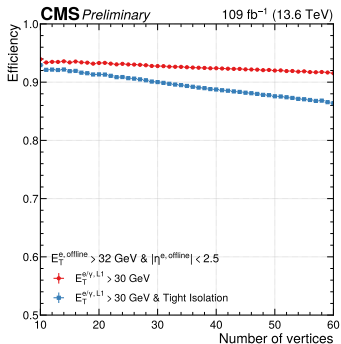
- ▶ Left: The L1T e/γ trigger efficiency as a function of the offline reconstructed E_T for three different high E_T thresholds on the Level-1 trigger e/γ candidate.
- ▶ Right: The L1T e/γ trigger efficiency as a function of the offline reconstructed E_T for two typical unprescaled algorithms, as well as their logical OR. The application and relaxation of the isolation requirement cause the blue curve's characteristic shape.

e/γ : Efficiency vs. p_T



- ▶ The L1T e/γ trigger efficiency as a function of the offline reconstructed E_T for three different low E_T thresholds on the L1T e/γ candidate, available in different cross-algorithms. The increase in plateau efficiency at $E_T \approx 30$ GeV is due to the E_T dependent HCAL over ECAL energy deposit fraction selection [1].

e/γ : Efficiency vs. Number of vertices



- ▶ The L1T e/γ trigger efficiency as a function of the number of offline reconstructed vertices, for both isolated and non-isolated candidates.

Hadronic tau lepton decays (τ_h)

L1T τ_h : Reconstruction & Identification

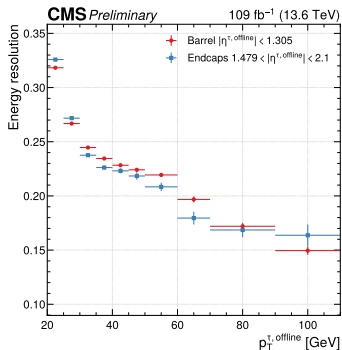
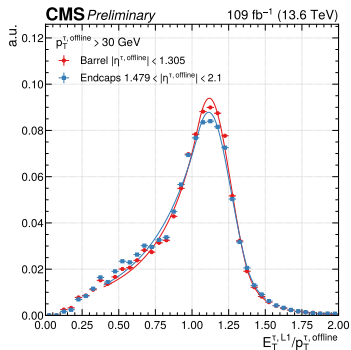
- ▶ The τ_h candidates are reconstructed starting from the same TT clusters used for the e/γ candidates (i.e. first two bullets of Slide 21).
- ▶ The τ_h candidates are subject to further merging under certain proximity conditions to account for the particle multiplicity of the hadronic decays.
- ▶ Isolation requirements are added to produce a collection of isolated τ_h objects. The isolation transverse energy E_T^{iso} corresponds to the energy deposit in a 6×9 TTs region in $\eta \times \phi$ around the seed TT, subtracting the candidate E_T . To determine if a candidate is isolated, a selection threshold is applied to E_T^{iso} depending on the candidate E_T , its η position, and a pileup estimator.
- ▶ The candidate E_T is then subject to further calibration, depending on the candidate E_T , its η position, and the possible presence of substantial EM contribution to the energy deposit.

L1T τ_h : Efficiency measurement

- ▶ The efficiency of the L1T τ_h trigger is measured using the tag-and-probe method and the following selections on offline-reconstructed muons and taus.

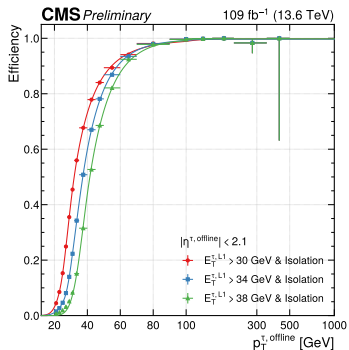
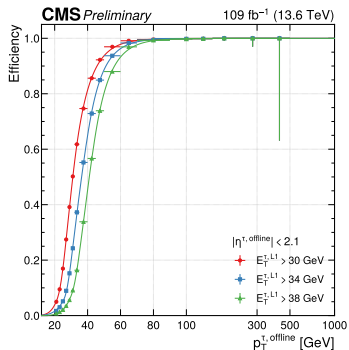
Tag muon	Probe tau	Tag-and-probe selection
$ \eta < 2.1$ Medium ID Matched to an isolated HLT muon firing the single-muon HLT path with threshold $p_T > 24 \text{ GeV}$ $\Delta R(\text{HLT}, \text{offline}) < 0.5$ $p_T > 24 \text{ GeV}$ Relative isolation < 0.1	$ \eta < 2.1$ DeepTau ID: Medium vsJet, Tight vsMu, Loose vsEle	$\Delta R(\text{tag}, \text{probe}) > 0.5$ $40 < m_{\text{tag+probe}}^{\text{visible}} < 80 \text{ GeV}$ $m_T < 30 \text{ GeV}$

τ_h : Energy response and resolution



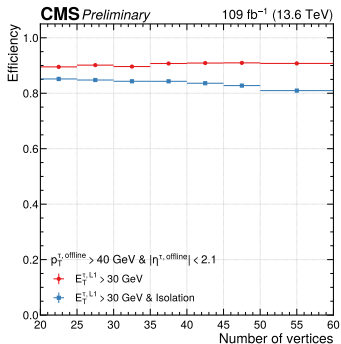
- ▶ Left: The L1T τ_h energy response with respect to the offline reconstructed p_T , separately for the barrel and endcap regions. The low response tail is due to the absence of calibration of the TTs in input to the L1 trigger τ reconstruction algorithm.
- ▶ Right: The L1T τ_h energy resolution, as a function of the $p_T^{\tau, \text{offline}}$, estimated by the root-mean-square of the $E_T^{\tau, L1} / p_T^{\tau, \text{offline}}$ distribution divided by its mean, in bins of $p_T^{\tau, \text{offline}}$.

τ_h : Efficiency vs. p_T



- ▶ Left: The L1T τ_h efficiency as a function of the offline reconstructed p_T for three typical thresholds on the Level-1 trigger τ candidate.
- ▶ Right: The L1T isolated τ_h efficiency as a function of the offline reconstructed p_T for three typical thresholds on the Level-1 trigger τ candidate.

τ_h : Efficiency vs. Number of vertices



- ▶ The L1T τ_h efficiency as a function of the number of offline reconstructed vertices, for both isolated and non-isolated candidates.

References

References

- [1] A.M. Sirunyan and et al. “Performance of the CMS Level-1 trigger in proton-proton collisions at $\sqrt{s} = 13$ TeV”. In: *Journal of Instrumentation* 15.10 (2020), P10017. DOI: {10.1088/1748-0221/15/10/P10017}.
- [2] CMS Collaboration. *Performances of L1 Jets and MET Trigger in early Run3*. CMS Detector Performance Note CMS-DP-2023-054. 2023. URL: <https://cds.cern.ch/record/2868796>.